In vivo CRISPR screens identify dual function of MEN1 in regulating tumor-microenvironment interactions

Peiran Su[1,2], Yin Liu[1,3], Francis Burrows[4], Ming S. Tsao[1,2], Housheng Hansen He[1,2]

1. Princess Margaret Cancer Center, University Health Network, Toronto, Ontario, Canada
2. Department of Medical Biophysics, University of Toronto, Toronto, Ontario, Canada
3. Department of Laboratory Medicine, Shanghai Pulmonary Hospital, Tongji University School of Medicine, Shanghai, China
4. Kura Oncology, San Diego, California, USA

Background

Functional genomic screens have been widely adopted to identify essential genes and potential drug targets in cell line models. However, it is well known that *in vitro* 2D cultured cell line models do not fully capture the biology in patient tumors due to the lack of the tumor microenvironment. The primary objective of this study was to perform functional genomic screens in *in vivo* models to identify clinically relevant epigenetic vulnerabilities.

Method

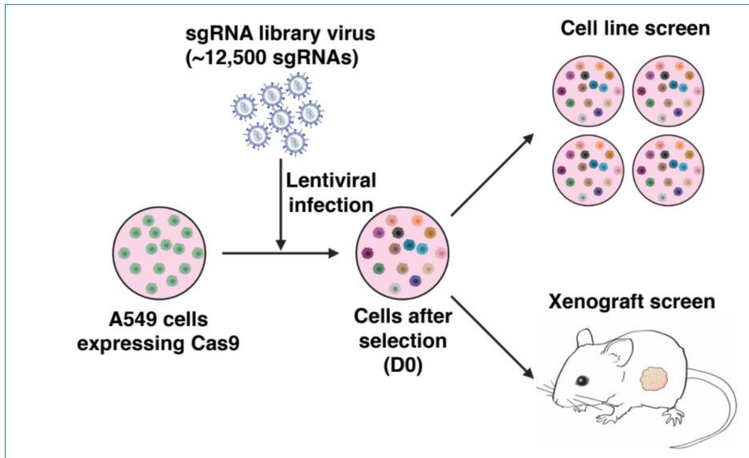

Figure 1: *In vitro* and *in vivo* CRISPR screening in lung cancer cell line A549. Schematic illustration of the CRISPR screening design. Lung cancer A549 cells with stable Cas9 expression were subject to *in vitro* cell line and *in vivo* xenograft screens in parallel. An in-house EpiDrug sgRNA library that target 317 epigenetic regulators and 650 genes with FDA approved drugs were used for the screening. Software MaGeCK and DrugZ were used to identify genes that confer differential essentialities *in vitro* and *in vivo*.

Results

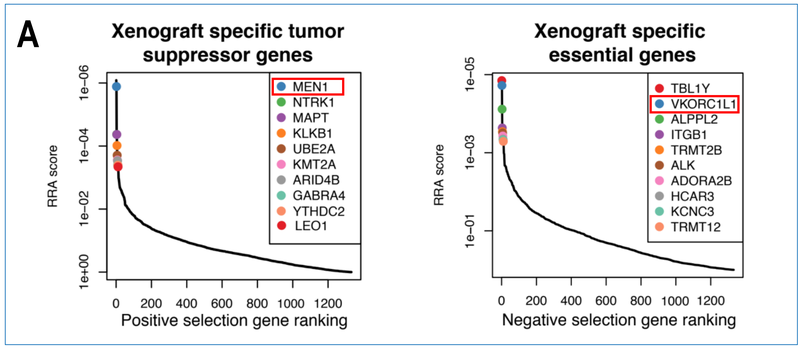

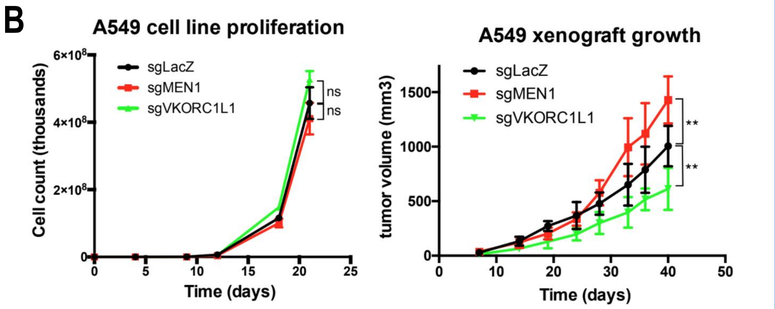

Figure 2: Identification and validation of *in vivo* specific targets through comparing *in vivo* and *in vitro* CRISPR screens in A549. **(A)**Top tumor suppressor (left) and essential (right) genes identified by CRISPR screen in A549 xenograft compared to 2D cultured cells. **(B)** Cell line (left) and xenograft growth curve (right) of A549 with and without knockout of MEN1 or VKORC1L1.

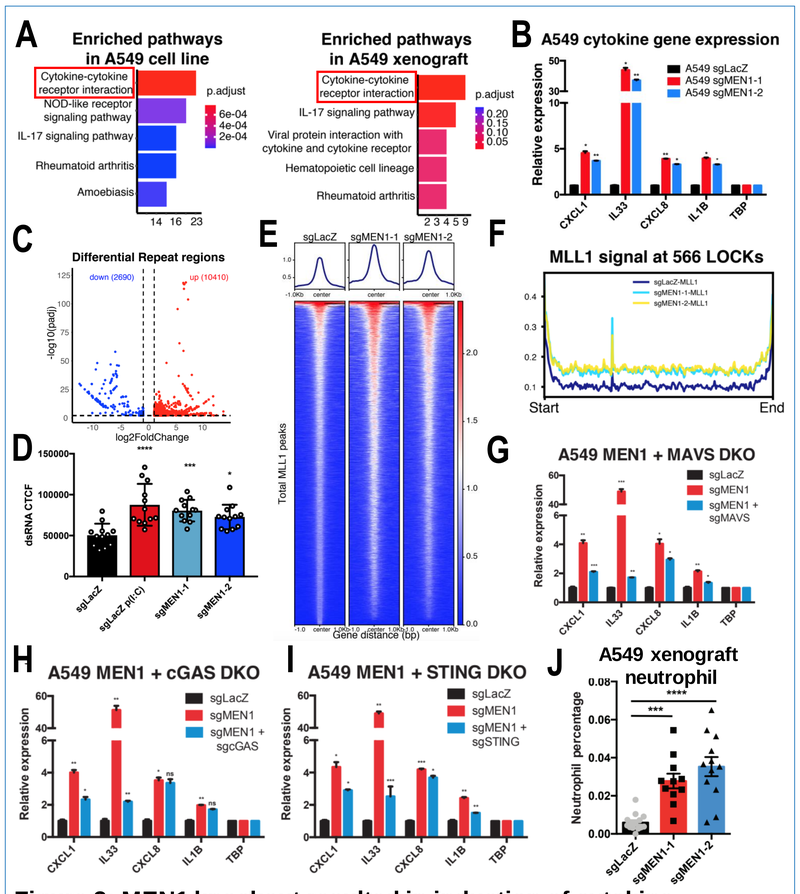

Figure 3: MEN1 knockout resulted in induction of cytokine production and dsRNA induced viral mimicry. (A) KEGG analysis of differential genes from MEN1 knockout A549 versus control *in vitro* (left) and *in vivo* (right). **(B)** RT-qPCR showing the relative expression of cytokine genes in MEN1 knockout A549 cells relative to control. **(C)** Volcano plot of repeat expression in A549 cells with and without knockout of MEN1. **(D)** Quantification of dsRNA fluorescence intensity in control, MEN1 knockout A549 cells or A549 cells treated with poly (I:C). **(E)** Heatmap showing MLL1 binding signal in A549 cells with and without knockout of MEN1. **(F)** Average profile of MLL1 binding signal at the LOCKs repeat regions. **(G-I)** qRT-PCR detection of selected cytokine genes abundancy in MAVS (G), cGAS (H) or STING (I) knockout A549 cells with and without silencing of MEN1. **(J)** Quantification of neutrophil infiltration in tumors with and without knockout of MEN1.

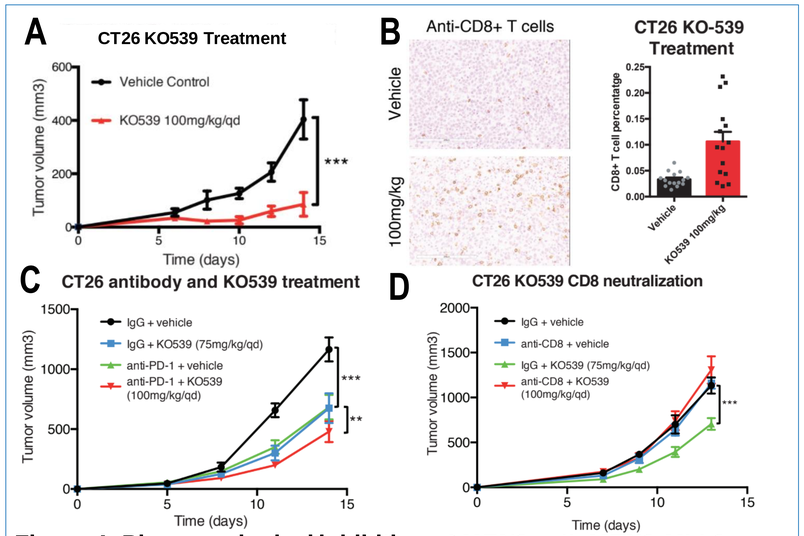

Figure 4: Pharmacological inhibition of MEN1 with MEN1-MLL1 inhibitor KO-539. (A) Tumor growth of CT26 treated with vehicle or KO-539. **(B)** Representative IHC images (left) and quantifications (right) of CD8⁺ T cell infiltration in CT26 tumors with and without KO539 treatment. **(C)** Tumor growth of CT26 treated with IgG or PD-1 antibody with and without treatment of KO539. (D) Tumor growth of CT26 treated with IgG or CD8 antibody with and without treatment of KO539.

Summary

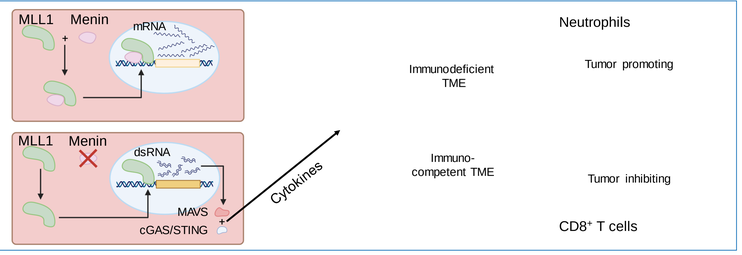

Acknowledgement

This work is supported by PMCF, CIHR and TFRI. We thank Kura Oncology for supplying KO-539 for this research.